2011

Experimental analysis of the surface roughness evolution of etched glass for micro/nanofluidic devices

Juan Ren
Iowa State University, juanren@iastate.edu

Baskar Ganapathysubramanian
Iowa State University, baskarg@iastate.edu

Sriram Sundararajan
Iowa State University, srirams@iastate.edu

CHAPTER 3. EXPERIMENTAL ANALYSIS OF THE SURFACE ROUGHNESS EVOLUTION OF ETCHED GLASS FOR MICRO/NANO FLUIDIC DEVICES

A paper published in *Journal of Micromechanics and Microengineering*

Jing Ren, Baskar Ganapathysubramanian and Sriram Sundararajan

Department of Mechanical Engineering, Iowa State University, Ames, IA 50011, USA

3.1 Abstract

Roughness of channel surfaces, both deterministic and random, is known to affect the fluid flow behavior in micro/nanoscale fluidic devices. This has relevance particularly for applications involving non-Newtonian fluids, such as in biomedical lab-on-chip devices. While several studies have investigated effects of relative large, deterministic surface structures on fluid flow, the effect of random roughness on micro fluid flow remains unexplored. In this study, the effects of processing conditions for wet etching of glass including etching time and etching orientation on central line average (Ra)a and the autocorrelation length (ACL) were investigated. Statistical distribution of the roughness was also studied. Results indicated that ACL can be tailored in the range of 1-4 μm by changing etching time in horizontal etching while Ra was found to increase weakly with etching time in all three etching orientations. Analysis of the experimental data using Kolmogorov-Smirnov goodness-of-fit hypothesis test (K-S test) shows that the glass surface roughness does not follow a Gaussian distribution, as is typically assumed in literature. Instead, the T location-scale distribution fits the roughness data with 1.11% error.

These results provide promising insights into tailoring surface roughness for improving micro-fluidic devices.

Keywords microfluidic device · surface roughness · autocorrelation length · surface height distribution · goodness-of-fit test

3.2 Introduction

Extensive studies during the past century indicate that surface roughness affects fluid flow behavior in microscale channels. Numerical simulations of micro flow in rough channels [1] showed that bulk flow velocity and the volumetric flow rate decrease in different rates as the roughness increases. Studies on the effect of surface roughness on friction force [2], pressure drop [3, 4], heat transfer in single-phase flow [5] and laminar-turbulent transition [6] indicate the necessity of precise control of the surface morphology inside the fluidic device for the purpose of enhancing the reliability and performance of the fluidic system [7]. Experimental results of blood flow in rough microchannels [8] emphatically showed that surface roughness affects blood viscosity due to boundary effects. Application of surface roughness for gradient generation in microfluidic system has also been widely studied [9-11].

In most of these studies, researchers relied on micro-machining or micro-fabrication techniques to produce deterministic roughness via designed shapes and patterns inside the microchannels. It is well known that almost all mechanical or chemical processing inherently produces random roughness on real surfaces [12] and consequently most engineering surfaces are random. However, the role of random roughness on microfluidic flow behavior remains

relatively unexplored. This aspect will become increasingly important as channel sizes continue to decrease in micro/nanofluidic applications.

In most microfluidic studies, surface roughness is described using only amplitude parameters such as relative roughness [1, 13, 14]. Spatial parameters such as autocorrelation length (ACL) or power spectral density function (PSDF) are rarely used. It is widely known that most important features of random surface roughness can be characterized by amplitude and spatial parameters [15]. Surfaces with identical amplitude parameters can have totally different topographical features that however can be characterized by differences in spatial parameters. A knowledge of both amplitude and spatial parameters can lead to methods to tailor random roughness [16].

The distribution of surface heights is another important aspect in surface roughness study. Surface height distribution is typically related to the nature of the processing method (Bhushan 2001). In most studies random roughness is assumed to possess a Gaussian or Uniform distribution [17-22]. Relatively few works attempt to experimentally verify this assumption for the processed surfaces involved. Zimmer et al. verified a Gaussian distribution for laser-induced backside wet etching on fused silica [23]. Suh and Polycarpou investigated the use of various density functions to describe textured surfaces in magnetic-storage devices [24]. Some chemically and mechanically processed surfaces were proved to be non-Gaussian and even anisotropic [25-28]. It has to be emphasized that the exact height distribution of random surfaces prepared for microfluidic devices has not been reported earlier.

In this paper, random roughness on glass substrates is created by chemical etching. Glass is one of the more important and common materials widely used in micro channel fabrication

[29]. Evolution of amplitude parameter Ra and spatial parameter ACL with etching time and orientation is investigated. Kolmogorov-Smirnov goodness-of-fit hypothesis test is used to verify the approximate distribution of the surface heights.

3.3 Experimental procedure

The surface roughness examined in this study was generated on glass slides (25 mm × 75 mm, Erie Scientific Company, Portsmouth, NH). The glass samples were etched by buffered HF (6:1 volume ratio of 40% NH4F in water to 49% HF in water) to generate different surface roughness. The etch rate was calibrated as 72 nm/min. Samples were immersed in buffered HF in three different orientations: horizontal, 45º and vertical. In each orientation, samples were prepared at several different etching times. Since the study is focused on how etching condition affects surface roughness for microfluidic applications, the glass surfaces etched by HF should be suitable for micro channel fabrication and further microfluidic experimental techniques, such as Particle Image Velocimetry (PIV), which requires superior channel transparency. Based on our experimental observation, etching times longer than 40 minutes in horizontal orientation resulted in significant surface damage on glass substrate, which led to difficulty in bonding during microchannel fabrication. Furthermore, transparency of the glass surface was significantly compromised. Therefore, in this study the maximum etching time reported is 40 minutes. Two samples were prepared for each etching condition. After HF etching, the samples were rinsed in DI water for 5 minutes and dried by nitrogen. Two smooth (un-etched) glass slides were also prepared for comparison.

An atomic force microscope (AFM, Dimension 3100, Nanoscope IV, Veeco Instruments, Santa Barbara) was used to measure surface roughness of the etched glass samples. All the

etched samples were cleaned in acetone and dried by nitrogen to remove organic waste and dust on the surface before taking AFM images. All the AFM scans were acquired in contact mode using a standard Si3N4 tip, at a scan resolution of 256×256 points. The scan size was chosen as 75 μm × 75 μm which is comparable to the common size of microchannels used for microfluidic study. Scan areas were chosen to avoid edges of the slides to ensure valid roughness information. As shown in figure 1, each slide was scanned by AFM from bottom to top in five areas to ensure the overall surface roughness information was obtained. Three AFM images were taken in each area, leading to 15 scans for each glass slide and 30 scans for each etching/orientation condition. The AFM surface height data was exported into MATLAB to analyze surface height distribution and to compute amplitude (Ra) and spatial (ACL) roughness parameters.

Figure 1. A schematic representing the scanned regions of each glass slide. Three AFM scans (75 μm × 75 μm) were acquired in each area to ensure roughness information was obtained over the entire slide.

Center line average (Ra) is the arithmetic mean of the absolute values of vertical deviation from the mean line of the profile which measures the relative departure of the profile in the vertical direction [30]. Ra is calculated as

$$Ra = \frac{1}{N}\sum_{i=1}^{N}|z_i - m| \tag{1}$$

where N is the number of total sampling points, z is the surface height, m is mean line of the surface profile.

Autocorrelation length (ACL) measures the degree of randomness of the surface roughness, and represents the distance over which two points can be treated as independent in a random process [31]. It is defined as the length over which the autocorrelation function decays to a small fraction of its original value. Many etched surfaces are widely assumed to produce an exponential autocorrelation function [30] given as

$$c(\tau) = \exp(-\tau/\beta) \tag{2}$$

where τ is the spatial separation. Autocorrelation length of this exponential autocorrelation function is defined as the distance at which value of the (τ) drops to $1/e$ of the initial value, which is equal to β [32].

Surface height distribution (fitting hypothesis) of the etched glass was validated by the Kolmogorov-Smirnov (K-S) goodness-of-fit test. Details of K-S test procedure are attached in appendix. Here we describe our rationale for sample size selection for the test. The size of the AFM surface roughness height data for each scan is 256×256. Usually, for small population sizes (<5000), a few dozen data are used for the K-S test. The standard K-S test was designed for

small sample sizes (~100) [33, 34]. Studies have verified that for very large populations, as is the case of our surface roughness data, the choice of sample size will have an effect on the test outcomes. As sample size decreases, goodness-of-fit test is less likely to perform poorly [35]. Determining the exact sample size needed for a given population size is still an open problem. In our study, 100 data was randomly collected from each experimental scan to run the test for both Gaussian and T location-scale fit. 1000 such tests were then executed for each scan to minimize the effect of any sampling bias. Confidence interval used in the test was 95%. Success rate of the 1000 tests was recorded.

3.4 Results and discussion

3.4.1 Surface roughness parameters

Representative AFM images obtained from horizontally etched glass surfaces are shown in Figure 2. Samples etched in the other two directions presented similar surface morphology changes as etching time increases up to 30 minutes. In horizontal etching, when etching time increases to 40 minutes, spreading holes and grooves appeared on the surface which drastically increase the Ra as shown in Figure 2. Noticeable side peaks appear in the AFM image indicating that the surface is becoming less isotropic. Samples became visibly rugged and dark in areas around the surface and were subsequently found to be unsuitable for microchannel fabrication due to poor transparency and bonding. In 45º etching, visible damage also occurred on the surfaces but was less severe. Interestingly, samples etched in vertical orientation did not exhibit this visible damage on the surface.

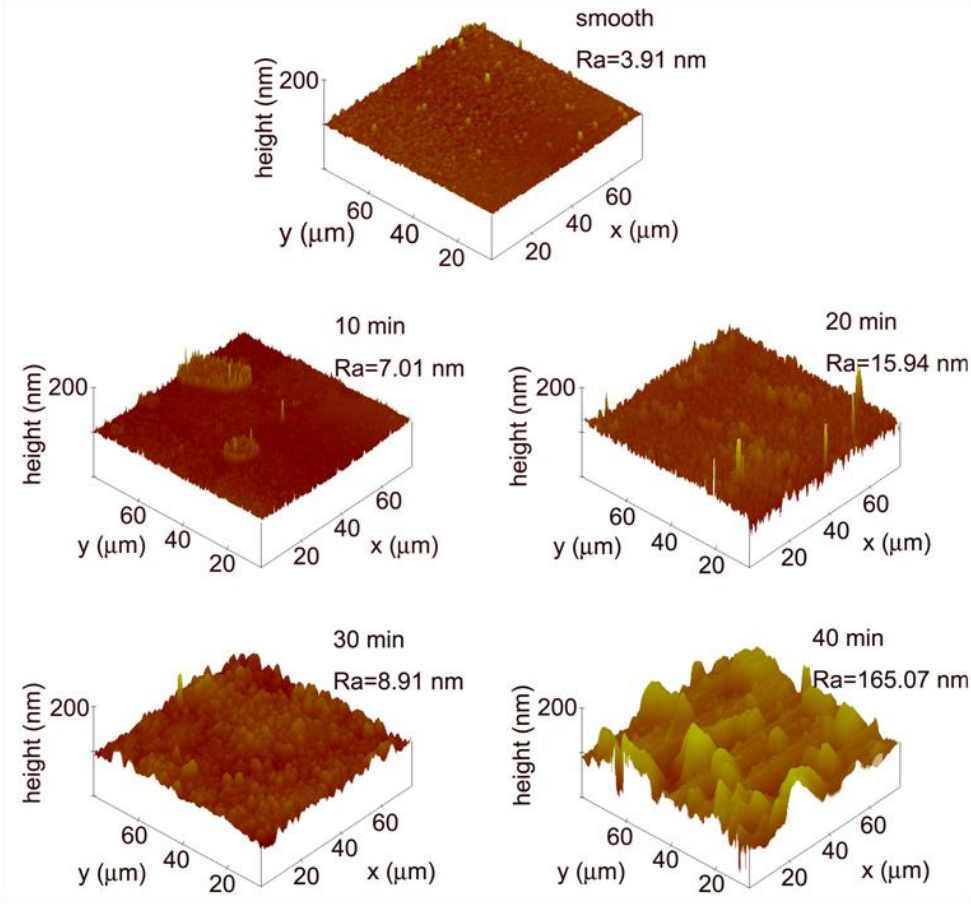

Figure 2. Representative AFM surface height images of horizontally etched glass. The surface morphology changes as etching time increases. When etching time increases to 40 minutes, the roughness increases drastically rendering the surface unsuitable for microchannel fabrication.

Center-line average

Figure 3 shows the effect of etching time on the amplitude parameter Ra for all three etching orientations.

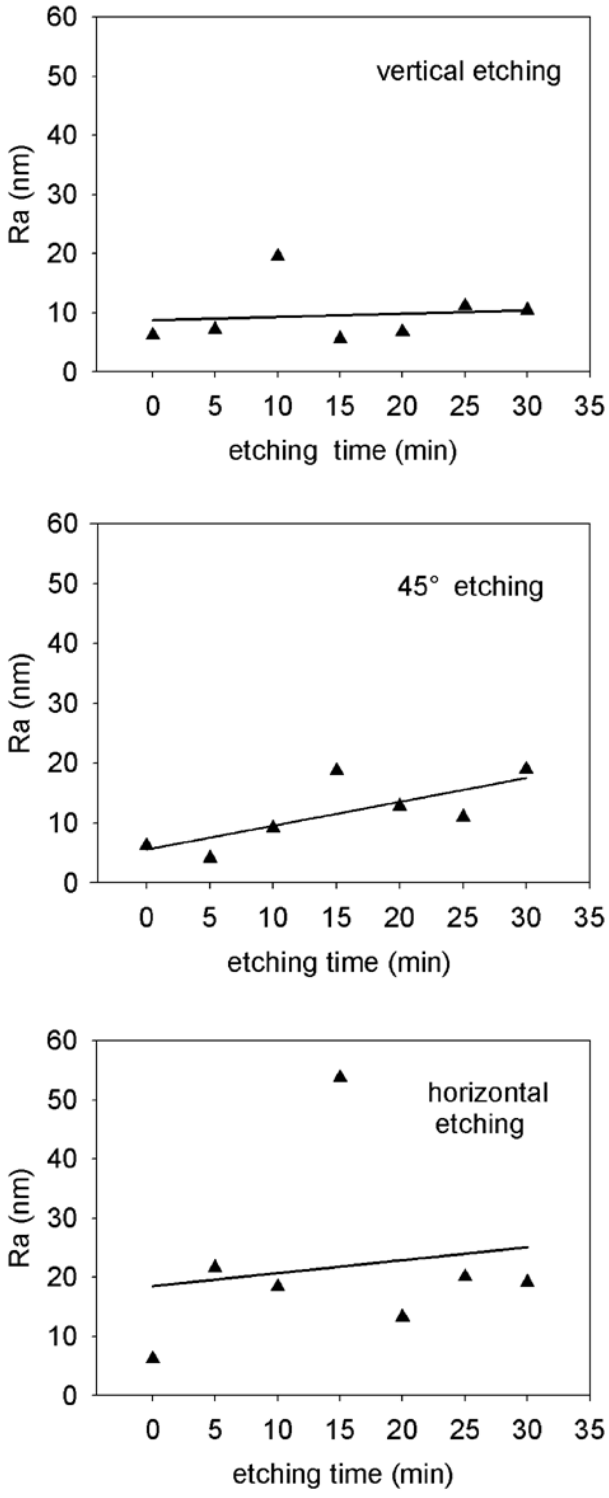

Figure 3. Variation of Ra with etching time in different etching orientations. The data suggest a slight increase of Ra with etching time. In 45º etching, Ra increases with etching time at a faster rate than in the other two orientations. However no strong trends were observed with regression analysis.

The data suggest a slight increase in Ra with etching time. Regression analysis indicated a stronger linear trend ($R^2 = 0.565 R^2 = 0.565$) for 45º etching, as compared to horizontal and vertical orientations ($R^2 < 0.1$ for both$R^2 < 0.1$forboth). The data suggest that generally higher variation in Ra values can be obtained by using horizontal etching, but precise tailoring is subtle under 30 minutes etching time. As discussed earlier, longer etching times resulted in substantial increase in Ra values and poor bonding during microchannel fabrication. For example, in horizontal etching, an etching time of 40 minutes results in a drastic increase in Ra to 149.14 nm compared to less than 60 nm for the other two etching orientations.

Autocorrelation length

Figure 4 shows the ACL evolution with etching time for the three different etching orientations. In vertical etching, ACL value appears to be independent of etching time in our time range. In 45º etching, linear regression shows a slight increase of ACL from 1 μm to 4 μm with etching time, while in horizontal etching, ACL value shows a much faster increase from 1 μm to 4 μm starting from 10 minutes. Therefore, as the etching orientation switching from vertical to horizontal gradually, ACL value shows increasingly obvious trend with etching time. According to the predicted behavior represented by the trend lines, ACL value can be tailored in the range of 1 μm to 4 μm in horizontal etching by controlling etching time.

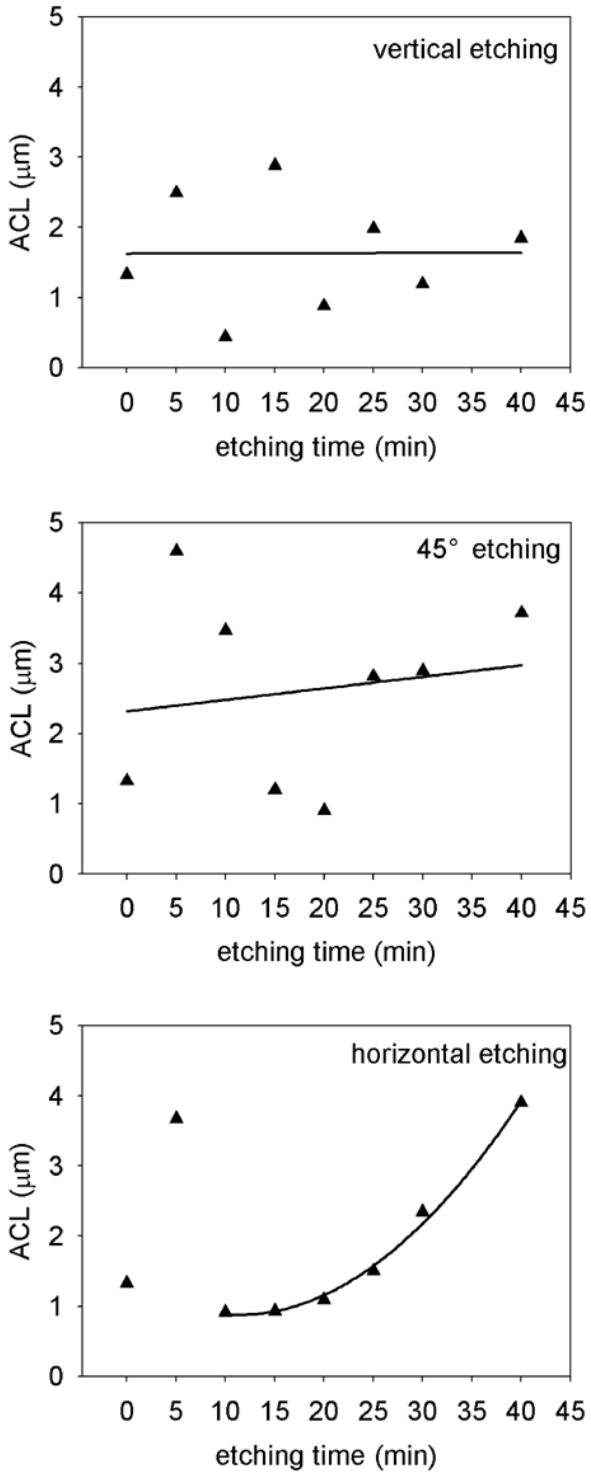

Figure 4. Variation of ACL with etching time in different orientations along with best-fit trend lines. In vertical etching, ACL value is independent of etching time. In 45º etching, ACL value shows a slight increase from 1 μm to 4 μm. In horizontal etching, the increasing behavior is more obvious.

3.4.2 Surface height distribution

Figure 5 shows representative histograms of AFM roughness height data at different etching times in horizontal etching. Statistical distribution of etched material surface has been assumed to be Gaussian in published literature [17, 18]. However, Figure 5 shows that the histogram of the AFM surface height data appears to be more heavy-tailed than Gaussian. We tried to describe the data with other distributions that fit leptokurtic data with heavy tails. T location-scale distribution is more appropriate than Gaussian distribution for modeling data with heavy tails, which is the case in the glass surface roughness height data. The probability density function of T location-scale distribution is defined as:

$$f(x)=\frac{\Gamma\left(\frac{\nu+1}{2}\right)}{\sigma\sqrt{\nu\pi}\,\Gamma\left(\frac{\nu}{2}\right)}\left[\frac{\nu+\left(\frac{x-\mu}{\sigma}\right)^2}{\nu}\right]^{-\left(\frac{\nu+1}{2}\right)} \tag{3}$$

where Γ is the gamma function, and μ, σ, and ν are mean, standard deviation and degree of freedom, respectively [36]. Figure 5 also shows both Gaussian and T location-scale fits for height data. It can be seen that compared with the Gaussian distribution, T location-scale distribution reproduces the data histogram much better in each case. The other two etching orientations also show similar behavior with the T location-scale showing a much better fit.

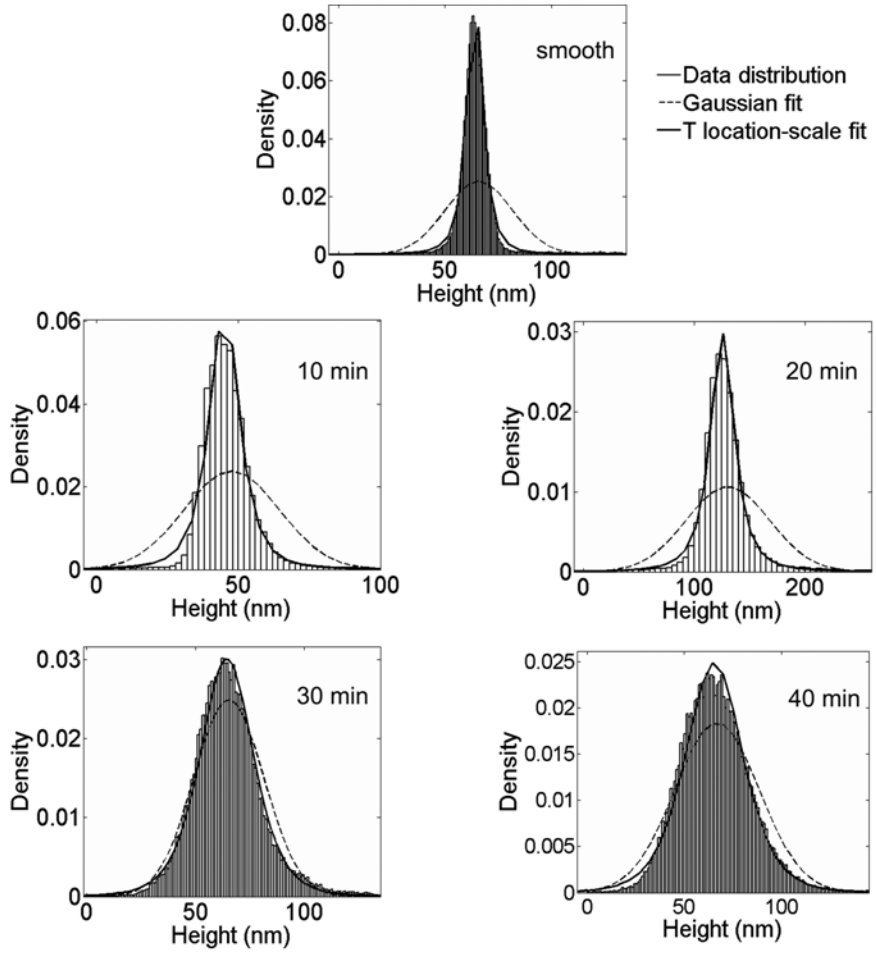

Figure 5. Histograms of the surface height data for horizontally etched glass surfaces at different etching times. Also shown are Gaussian and T location-scale fits of the data. T location-scale distribution fits the data better than Gaussian distribution.

In order to verify the hypothesis that the AFM surface height data follows a T location-scale distribution rather than a Gaussian distribution, the Kolmogorov-Smirnov (K-S) goodness-of-fit test was executed on both fitted distributions. Result of the test showed average success rate of Gaussian distribution fitting to be 0, which means Gaussian distribution fails to fit any of the surface roughness height data. In contrast, the average success rate of T location-scale distribution fitting was 95.5%, indicating an excellent fit between a T location-scale distribution and the experimental data at a 95% confidence interval.

For each data set, an error which is defined as the discrepancy between the empirical cumulative distribution function (CDF) and theoretical CDF of T location-scale distribution, was computed. Figure 6 (a) shows this error of a representative AFM roughness height data set. It can be seen that the error is less than 2.5%. Figure 6 (b) shows the histogram of average fitting error for all the 617 experimental data sets. The average fitting error is about 1.11% while most of the error is less than 2%, which validates the T location-scale distribution as a good fit to the surface height data.

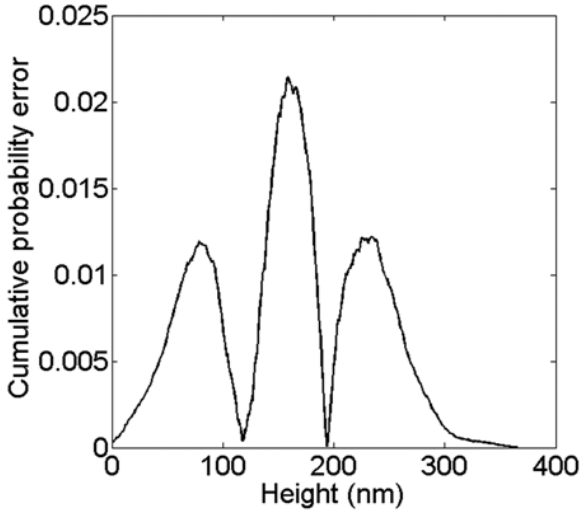

(a)

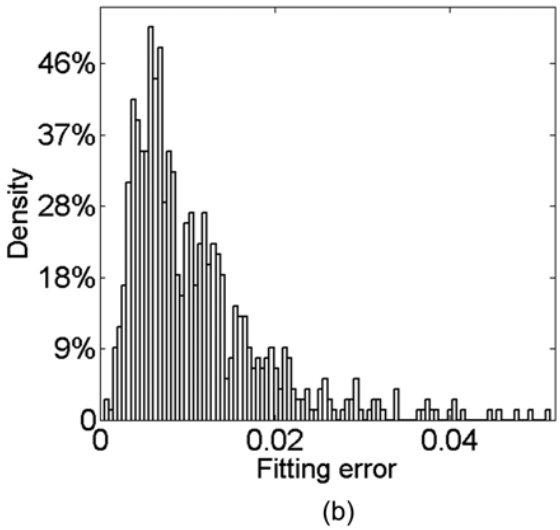

(b)

Figure 6. Error between empirical CDF of the surface roughness height data and theoretical CDF of a T location-scale distribution: (a) error for one experimental data set; (b) histogram of fitting error for all the 617 experimental data sets.

3.5 Conclusions

In this paper, surface roughness was generated on glass substrate by buffered HF etching and measured by Atomic Force Microscopy. Evolutions of roughness parameters Ra and ACL were characterized as function of etching time and orientation. In addition, the height distribution of the etched glass surface was also analyzed.

The etching orientation of the glass slides affects the evolution of the roughness in addition to etching time. Spatial parameter ACL increases roughly from 1 μm to 4 μm in both 45º and horizontal etching. ACL value shows a weak linear increase with time in 45º etching, and a much faster and predictive increase in horizontal etching, while vertical etching has no discernible effect. This evolution behavior provides a potential way to tailor the random roughness of glass surface in HF etching by controlling etching time and orientation simultaneously. The amplitude parameter Ra shows a weak linear increase with etching time in all etching orientations.

Analysis of the height distribution showed that the etched glass surfaces were non-Gaussian. Instead, a T location-scale distribution was demonstrated to fit the AFM surface height data. In addition, for large data set modeling, the effect of sample size selection on the outcome of goodness-of-fit test needs to be examined.

Evolution of surface roughness with etching time and orientation brings insights into the possibility of tailoring random roughness for designed microfluidic flow performances.

Furthermore, the surface height distribution studied in this paper provides a basis for modeling and analysis of random rough surface and simulations of fluid flow in microscale rough channels.

Current and future work on this study will be to extend surface roughness analysis of other pertinent materials for microfluidic device fabrication, such as silicon, as well as assessing the impact of random roughness on laminar microfluidic flow using particle image velocimetry (PIV) technique [37].

3.6 Acknowledgement

The authors would like to thank Chris Tourek, a Mechanical Engineering graduate student at Iowa State University for assistance with using the AFM in this study.

3.7 Appendix

K-S test is widely used to decide if a sample comes from a population with a specific distribution [38]. It is based on testing the maximum distance between the empirical cumulative distribution function (empirical CDF) and the theoretical cumulative distribution function (theoretical CDF). If the AFM surface height data follows a certain distribution, the empirical CDF is expected to be very close to the theoretical CDF of the specified distribution, e.g. T location-scale distribution. If the distance is not small enough, the hypothesis that the data follows the specific distribution will be considered incorrect and rejected. The test was executed on both Gaussian and T location-scale fitting.

Process of Kolmogorov-Smirnov test for AFM surface height data:
H_0: The height data is drawn from T location-scale distribution.
Ha: The height data is not drawn from T location-scale distribution.

Test Statistic: the Kolmogorov-Smirnov test statistic is defined as $D_n = \sup_x |S_n(x) - F_x(x)|$ $D_{n,m} = sup|S_m(x) - S_n(x)|$, where $S_n(x) S_m(x)$ is the empirical CDF of the sample and $S_n(x)$ is theoretical CDF.

Significance level: $\alpha = 0.05$. If D_n does not exceed the critical value, the null hypothesis is true and we can conclude that the height data is drawn from the expected distribution. If D_n exceeds the critical value, the null hypothesis is rejected.

3.8 References

1. Yang, D.Y. and Y. Liu, *Numerical simulation of electroosmotic flow in microchannels with sinusoidal roughness.* Colloids and Surfaces a-Physicochemical and Engineering Aspects, 2008. **328**(1-3): p. 28-33.

2. Palasantzas, G. and A. Widom, *Roughness effects on the sliding frictional force of submonolayer liquid films on solid substrates.* Physical Review B, 1998. **57**(8): p. 4764-4767.

3. Kandlikar, S.G., et al., *Characterization of surface roughness effects on pressure drop in single-phase flow in minichannels.* Physics of Fluids, 2005. **17**(10).

4. Bahrami, M., M.M. Yovanovich, and J.R. Culham, *Pressure drop of fully developed, laminar flow in rough microtubes.* Journal of Fluids Engineering-Transactions of the Asme, 2006. **128**(3): p. 632-637.

5. Kandlikar, S.G., S. Joshi, and S.R. Tian, *Effect of surface roughness on heat transfer and fluid flow characteristics at low reynolds numbers in small diameter tubes.* Heat Transfer Engineering, 2003. **24**(3): p. 4-16.

6. Hao, P.F., et al., *Experimental investigation of water flow in smooth and rough silicon microchannels.* Journal of Micromechanics and Microengineering, 2006. **16**(7): p. 1397-1402.

7. Komvopoulos, K., *Surface engineering and microtribology for microelectromechanical systems.* Wear, 1996. **200**(1-2): p. 305-327.

8. Prentner, S., et al., *Effects of Channel Surface Finish on Blood Flow in Microfluidic Devices.* Dtip 2009: Symposium on Design, Test, Integration and Packaging of Mems/Moems, 2009: p. 51-54

429.

9. Kang, T., J. Han, and K.S. Lee, *Concentration gradient generator using a convective-diffusive balance.* Lab on a Chip, 2008. **8**(7): p. 1220-1222.

10. Keenan, T.M. and A. Folch, *Biomolecular gradients in cell culture systems.* Lab on a Chip, 2008. **8**(1): p. 34-57.

11. Lin, F., et al., *Generation of dynamic temporal and spatial concentration gradients using microfluidic devices.* Lab on a Chip, 2004. **4**(3): p. 164-167.

12. Thomas, T.R., *Rough surfaces*. 1999: Imperial College Press.

13. Taylor, J.B., A.L. Carrano, and S.G. Kandlikar, *Characterization of the effect of surface roughness and texture on fluid flow - past, present, and future.* International Journal of Thermal Sciences, 2006. **45**(10): p. 962-968.

14. Rawool, A.S., S.K. Mitra, and S.G. Kandlikar, *Numerical simulation of flow through microchannels with designed roughness.* Microfluidics and Nanofluidics, 2006. **2**(3): p. 215-221.

15. Hu, Y.Z. and K. Tonder, *Simulation of 3-D Random Rough-Surface by 2-D Digital-Filter and Fourier-Analysis.* International Journal of Machine Tools & Manufacture, 1992. **32**(1-2): p. 83-90.

16. Zhang, Y.L. and S. Sundararajan, *Method to generate surfaces with desired roughness parameters.* Langmuir, 2007. **23**(16): p. 8347-8351.

17. Lu, J.Q., A.A. Maradudin, and T. Michel, *Enhanced backscattering from a rough dielectric film on a reflecting substrate.* Journal of the Optical Society of America B-Optical Physics, 1991. **8**(2): p. 311-318.

18. Payne, A.P. and B.M. Clemens, *Influence of Roughness Distributions and Correlations on X-Ray-Diffraction from Superlattices.* Physical Review B, 1993. **47**(4): p. 2289-2300.

19. Lin, G., C.-H. Su, and G.E. Karniadakis, *Random Roughness Enhances Lift in Supersonic Flow.* Physical Review Letters, 2007. **99**(10): p. 104501.

20. Lin, G., C.H. Su, and G.E. Karniadakis, *Stochastic modeling of random roughness in shock scattering problems: Theory and simulations.* Computer Methods in Applied Mechanics and Engineering, 2008. **197**(43-44): p. 3420-3434.

21. Tartakovsky, D.M. and D. Xiu, *Stochastic analysis of transport in tubes with rough walls.* Journal of Computational Physics, 2006. **217**(1): p. 248-259.

22. Ganapathysubramanian, B. and N. Zabaras, *Sparse grid collocation schemes for stochastic natural convection problems.* Journal of Computational Physics, 2007. **225**(1): p. 652-685.

23. Zimmer, K., R. Bohme, and B. Rauschenbach, *Using IR laser radiation for backside etching of fused silica.* Applied Physics a-Materials Science & Processing, 2007. **86**(3): p. 409-414.

24. Suh, A.Y. and A.A. Polycarpou, *Modeling of the effect of preferential texturing on the interfacial forces in sub-5 nm ultralow flying head-disk interfaces.* Journal of Tribology-Transactions of the Asme, 2007. **129**(3): p. 553-561.

25. Chilamakuri, S.K. and B. Bhushan, *Contact analysis of non-Gaussian random surfaces.* Proceedings of the Institution of Mechanical Engineers Part J-Journal of Engineering Tribology, 1998. **212**(J1): p. 19-32.

26. Lee, H.J., Y.B. Chen, and Z.M. Zhang, *Directional radiative properties of anisotropic rough silicon and gold surfaces.* International Journal of Heat and Mass Transfer, 2006. **49**(23-24): p. 4482-4495.

27. Zhu, Q.Z. and Z.M. Zhang, *Anisotropic slope distribution and bidirectional reflectance of a rough silicon surface.* Journal of Heat Transfer-Transactions of the Asme, 2004. **126**(6): p. 985-993.

28. Zhu, Q.Z.Z. and Z.M.M. Zhang, *Correlation of angle-resolved light scattering with the microfacet orientation of rough silicon surfaces.* Optical Engineering, 2005. **44**(7): p. -.

29. Zhang, X.L. and S.J. Haswell, *Materials matter in microfluidic devices.* Mrs Bulletin, 2006. **31**(2): p. 95-99.

30. Bhushan, B., *Modern tribology handbook*. Vol. 1. 2001, Boca Raton: CRC.

31. Zhang, Y.L. and S. Sundararajan, *The effect of autocorrelation length on the real area of contact and friction behavior of rough surfaces.* Journal of Applied Physics, 2005. **97**(10): p. -.

32. Whitehouse, D.J. and J.F. Archard, *The Properties of Random Surfaces of Significance in their Contact.* Proceedings of the Royal Society of London. Series A, Mathematical and Physical Sciences, 1970. **316**(1524): p. 97-121.

33. Ajiferuke, I., D. Wolfram, and F. Famoye, *Sample size and informetric model goodness-of-fit outcomes: a search engine log case study.* Journal of Information Science, 2006. **32**(3): p. 212-222.

34. Strum, D.P., J.H. May, and L.G. Vargas, *Modeling the uncertainty of surgical procedure times - Comparison of log-normal and normal models.* Anesthesiology, 2000. **92**(4): p. 1160-1167.

35. Zhu, B.P., et al., *Factors affecting the performance of the models in the mortality probability model II system and strategies of customization: A simulation study.* Critical Care Medicine, 1996. **24**(1): p. 57-63.

36. J. K. Ghosh, M.D., Tapas Samanta, *An introduction to Bayesian analysis: theory and methods*. 2006: Springer.

37. Ren, J., et al. *Effect of channel surface roughness on microfluidic flow velocity*. in *47th Annual Technical Meeting of Society of Engineering Science*. 2010. Ames, IA.

38. Massey, F.J., *The Kolmogorov-Smirnov Test for Goodness of Fit.* Journal of the American Statistical Association, 1951. **46**(253): p. 68-78.